Typical Bearing-Fault Rating Using Force Measurements-Application to Real Data

Janko Slavič[1], Aleksandar Brković[1,2], Miha Boltežar[1]

August 10, 2012

[1]Laboratory for Dynamics of Machines and Structures, Faculty of Mechanical Engineering, University of Ljubljana, Aškerčeva 6, 1000 Ljubljana, Slovenia - EU.
[2]Faculty of Mechanical Engineering, University in Kragujevac, Sestre Janjic 6, 34000 Kragujevac, Serbia

Cite as:
J. Slavič, A Brković and M. Boltežar
Typical bearing-fault rating using force measurements: application to real data. Journal of Vibration and Control, December 2011 vol. 17 no. 14 2164-2174.. DOI: 10.1177/1077546311399949

Abstract

In contrast to the commonly used acceleration measurement, this research discusses the use of force measurements to identify bearing faults. A force sensor is fixed between the rigid surroundings and the bearing to measure all the reactive forces due to the vibration excitation.
Using a force measurement, systematically prepared samples with the five typical faults that can occur during the assembly process (axial, radial, bending moment, contamination and shield defect) were investigated. The samples were prepared with low, medium and high fault rating. The force measurement, with its relatively simple signal processing based on an envelope detection, was shown to be successful in correctly identifying both the fault rating and the fault type.
The presented approach was successfully applied to high-series assembly production and is relatively easy to apply to similar applications.

1 Introduction

Bearings are one of the most common elements in rotating machinery, and as a consequence, bearing failure is also one of the primary causes of breakdown in rotating equipment. The robustness and reliability of the bearings are essential qualities for the health of a machine. Defects in bearings may arise during

use or during the manufacturing process. Therefore, the detection of these defects is important for condition monitoring as well as the quality inspection of bearings. Different methods are used for the detection and diagnosis of bearing defects; Kim and Lowe [1] broadly classified them as vibration and acoustic measurements, temperature measurements and wear-debris analysis. Among these, vibration measurements are the most widely used. Tandon and Choudhury [2] presented a detailed review of the different vibration and acoustic methods for the condition monitoring of roller bearings, such as vibration measurements in the time and frequency domains, the shock-pulse method, sound pressure and the sound-intensity method.

Ho and Randall [3] showed that when a fault on one surface of a bearing strikes another surface, a force impulse is generated that excites resonances in the bearing and the machine. The successive impacts produce a series of impulse responses as a result of the passage of the fault through the load zone. The impulse response is usually measured by an acceleration, velocity or displacement sensor and the analysis of the vibration signal with amplitude modulation is usually based on the high-frequency resonance technique called envelope analysis. With envelope analysis the defect frequency is separated from the natural frequency excited by impact. In short, an envelope analysis is based on demodulation and consists of band-pass filtering and the Hilbert transform. This technique has been used extensively and its success has been demonstrated by several investigators. A review of this technique has been presented by McFadden and Smith [4].

McFadden and Smith [5, 6] investigated the way in which the bearing-fault signal (shown as a displacement rather than an acceleration) is manifested in the envelope spectrum and they developed a single-mode vibration model to explain the appearance of various spectral lines relating to different locations in the demodulated spectrum. This model was extended by Su and Lin [7] to characterize the vibrations of bearings that were subjected to a variety of loadings. A method of fault-feature extraction based on an intrinsic mode function was recently investigated by Yang et al. [8] to overcome the limitations of the conventional envelope-analysis method. Guo et al. [9] proposed a method for bearing-fault diagnosis based on the Hilbert transform, the envelope spectrum and the support vector machine. Furthermore, Sheen [10] developed a least-squares method for envelope extraction and used a logarithmic transformation to enhance the amplitude difference between the spectra of a defect bearing and a normal one.

In real applications the impulses generated inside the bearing are distorted by other sources of vibration. Randall [11] investigated a complex vibration signal from helicopter gearboxes and reported signals' acquisition difficulties with externally mounted accelerometers, because the bearing signals cannot avoid being mixed with the gear signals. Mendel et al. [12] presented a comprehensive case of acceleration measurements on rotating machines from oil rigs. They showed that the machine structure and the position of the acceleration sensors can influence the bearing vibrations to become more complex because of a lot of random vibration components from other parts of the machine.

In addition to the well-established signal-processing methods, fault identification has been well researched in the past decade. Among others, Yang *et al.* [13] used a higher-order spectral analysis for the diagnosis of the condition of motor bearings, and a bispectral analysis for fault identification in rotating machinery was performed by Wang *et al.* [14] and others [15]. Promising results for fault identification were obtained by using the continuous wavelet transform by Boltežar *et al.* [16] and others [17, 18, 19]. Abbassion *et al.* [20] researched the bearing fault clasification based on the wavelet transform and support vector machine; similarly, Guo *et al.* [9] researched the Hilbert transform and support vector machine for fault clasification of bearings. Multi-resolution analyses and neural networks have also been used for the identification of bearings [21, 22].

Despite the progress in signal-processing methods, ball-bearing manufacturers still tend to use the standard Anderon Meter made by Sugawara Laboratories. This machine measures noise with an accelerometer contacting the outer race of the bearing while the inner race is rotated. The noise levels are separated into three bands (low, medium and high).

Instead of measuring the acceleration, this study focuses on measuring the force. The reason is that when the acceleration is measured, the bearings' perfect fixation would be free-free to avoid uncertainties due to boundary conditions; however, the bearing is usually fixed and the vibrations (amplitude and frequency) are influenced by the fixation. In this research the bearing is fixed directly to the force sensor and all the vibrations go through the force sensor. It is shown that relatively simple signal processing can be used to reliably identify the fault rating and also to identify the fault type.

As well as the force measurement method, the contribution of this research is a systematic case-study research of typical bearing faults: axial, radial, bending moment, contamination and a shield defect. For each case, mechanical loads were introduced at three levels: low, medium and high. The main goal of this research was to determine whether it is possible to identify the most common manufacturing faults and their rating in ball bearings by using a force measurement.

The paper is organized as follows: In Section 2, the theoretical background for a vibration analysis of bearing faults is described. The experimental setup and the test rig used in this research are described and illustrated in Section 3. Section 4 presents the obtained results and comparisons of the bearing fault rating. The conclusions are drawn in Section 5.

2 Theoretical background

It was shown by Randall [23] that a frequency analysis of raw signals does not provide the desired diagnostic information, whereas the frequency spectra of the envelope signals do provide this information. The focus of this research is a force-based measurement approach and therefore the envelope analysis as a classical approach to bearing-fault identification is used. For the sake of brevity, only a basic theoretical background to envelope analysis is given in this section;

for details the reader should refer to [24].

2.1 Fault models in bearings

Defective bearings present characteristic frequencies depending on the localization of the defect [4]. There are five characteristic frequencies related to different fault locations. They are the shaft rotational frequency f_s, the fundamental cage frequency f_c, the ball pass inner raceway frequency f_i, the ball pass outer raceway frequency f_o and the ball spin frequency f_{bs}. Note that the ball spin frequency f_{bs} is the frequency with which the fault strikes the same race (inner or outer), so that in general there are two impacts per basic period. If these impacts (or at least their envelopes) were identical, the odd harmonics would vanish and the fundamental frequency would be twice f_{bs}, called the rolling element frequency f_{re} [11]. The characteristic fault frequency can be calculated using the following equations [2, 11]:

$$f_c = \frac{1}{2} f_s (1 - \frac{D_b}{D_m} \cos\theta) \tag{1}$$

$$f_i = \frac{N_b}{2} f_s (1 + \frac{D_b}{D_m} \cos\theta) \tag{2}$$

$$f_o = \frac{N_b}{2} f_s (1 - \frac{D_b}{D_m} \cos\theta) \tag{3}$$

$$f_{bs} = f_s \frac{D_m}{2D_b} (1 - \frac{{D_b}^2}{{D_m}^2} \cos^2\theta) \tag{4}$$

where D_b is the ball diameter, D_m is the mean diameter, θ is the load angle based on the ratio of the axial to the radial load[1] and N_b is the number of balls, see Figure 1. These equations assume that the rolling elements do not slide, but roll over the race's surfaces. However, as was shown by Randall [23], in reality there is always some slip and these equations give a theoretical estimate that would vary by 1-2% from the actual values.

The frequencies given by Equations (1)-(4) will only be present in the vibration spectrum when the bearings are really defective or, at least, when their components are subject to stress and deformations that can induce a fault.

2.2 Envelope analysis

As was mentioned in the introduction, in this study the envelope-detection method was used to identify the characteristic fault frequency given by Equations (1)-(4). As presented in Figure 2, the first step in the envelope-detection method is signal filtering with a band-pass filter (see Figure 2c) around the highest peak chosen from the spectrum of a raw signal in a high-frequency region,

[1] To increase the reliability of operation the radial bearings are usually axially prestressed with a relatively small force.

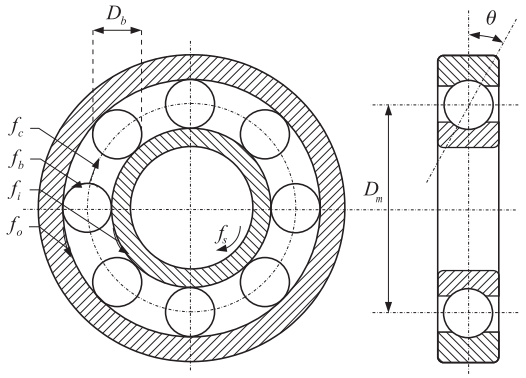

Figure 1: Ball-bearing structure and characteristic frequencies

see Figure 5b. This eliminates the frequencies associated with low-frequency defects (for instance unbalance and misalignment, see Figure 2b and 2d) and eliminating noise. This band-pass filtered signal is then demodulated using the Hilbert transform (Figure 2e), in which the signal is rectified and smoothed. The spectrum of the envelope signal (Figure 2f) in the low-frequency range is then obtained to determine the characteristic defect frequency of the bearing. With this analysis it is possible to identify not only the occurrence of the faults in bearings, but also to identify possible sources, like faults in the inner and outer race, or in the rolling elements [25].

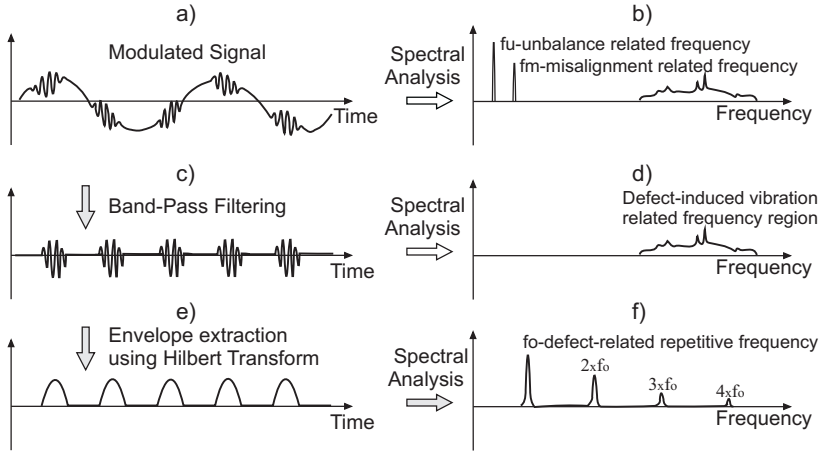

Figure 2: Procedure for envelope analysis based on band-pass filtering and the Hilbert transform

2.3 Hilbert transform

The Hilbert transform represents a standard technique for forming a signal's envelope. While a discussion of the Hilbert transform theory [26] is beyond the scope of this paper, a basic mathematical formulation for envelope extraction will be given here. Mathematically, the Hilbert transform of a real-valued signal $x(t)$ is defined as:

$$\tilde{x}(t) = \mathcal{H}[x(t)] = \frac{1}{\pi} \int_{-\infty}^{\infty} \frac{x(\tau)}{t-\tau} \, \mathrm{d}\tau \tag{5}$$

where $\mathcal{H}[\cdot]$ denotes the Hilbert transform operator. The symbol $\tilde{x}(t)$ represents a real-valued signal, and can be considered as the convolution of $x(t)$ and $\frac{1}{\pi\, t}$.

According to the convolution theorem, the Fourier transform of the convolution of two signals is the product of the respective Fourier transform of the two signals. Accordingly, the Fourier transform of $\tilde{x}(t)$ can be expressed as:

$$\tilde{X}(f) = X(f) \times \mathcal{F}\left[\frac{1}{\pi\, t}\right] \tag{6}$$

where the symbol $\times$ denotes the product operator, $\mathcal{F}[\cdot]$ denotes the Fourier transform operator, and $X(f)$ is the Fourier transform of the signal $x(t)$. The Fourier transform of $\frac{1}{\pi\, t}$ is given by:

$$\mathcal{F}\left[\frac{1}{\pi\, t}\right] = -j\,\mathrm{sign}(f) = \begin{cases} -j, & f > 0 \\ 0, & f = 0 \\ j, & f < 0 \end{cases} \tag{7}$$

Therefore, the Hilbert transform can be viewed as a filter of amplitude unity and phase $\pm 90°$, depending on the sign of the frequency of the input signal spectrum.

The real signal $x(t)$ and its Hilbert transform $\tilde{x}(t)$ can form a new complex signal, which is called the analytical signal, defined as:

$$z(t) = x(t) + j\,\tilde{x}(t). \tag{8}$$

The modulus of the complex signal $z(t)$ represents its envelope $e(t)$:

$$e(t) = ||z(t)|| = \sqrt{x(t)^2 + \tilde{x}(t)^2} \tag{9}$$

This indicates that performing the Hilbert transform on a real-valued signal leads to the formulation of a corresponding analytic signal, the magnitude of which is the envelope of the real signal, see Figure 3a. By performing a FFT on the envelope signal $e(t)$, the spectrum of the envelope can be obtained and used as a reliable source of information for bearing diagnostics, see Figure 3b [3]. In this research each mechanical fault was introduced at three levels: low, medium and high. In the Experiment section it will be shown that the envelope method successfully identifies the fault even at low levels of faults.

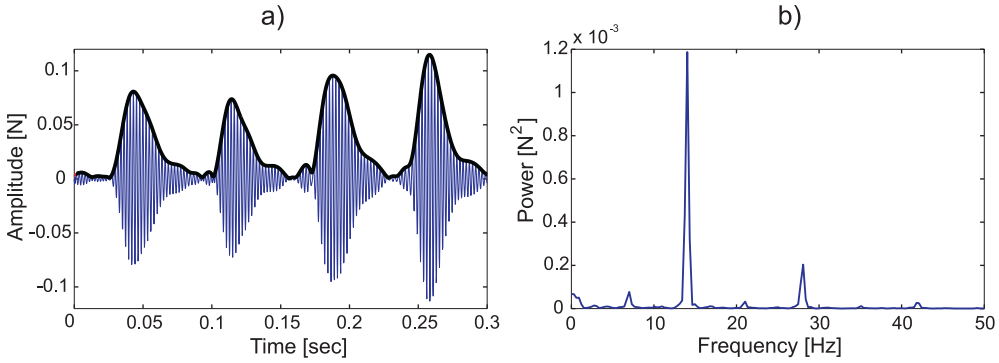

Figure 3: Axially loaded bearing signal: a) filtered and demodulated, b) envelope power spectrum

3 Experiment

3.1 Experimental setup

Figure 4 shows the experimental setup. The axial bearing is, on one side, fixed to the three-axial force sensor and, on the other side, to a rotating mass of 115 grams. Due to gravity the rotating mass pre-stresses the bearing and therefore the rotating bearing balls are in contact with the inner and outer races.

With the Kistler Type 9317B piezo-electric force sensor, dynamical forces from a few mN up to one N were measured in the x, y and z directions. The electrically commutated drive-motor with passive control was used to speed up the rotating mass and to keep the rotating velocity constant during the measurement. To avoid mechanical coupling, the drive and the rotating mass were touching only slightly via a soft, cotton-based joint, see Figure 4.

For example, Figure 5a shows a typical axial force measurement. It can be clearly seen that a force impact due to the passage of the fault through the load zone result in the damped natural response of the dynamical system with the bearing.

For the results in the Figure 5 the sample was rotating at 4 Hz and for the new bearing as well as for the bearing with axial fault a natural frequency around 450Hz was observed. If the rotating mass was increased to 250g, then this natural frequency decreased to approximately 350Hz. The natural frequency was found constant with the frequency of rotation (i.e. no nonlinear effects depending on the frequency of rotation were observed).

3.2 Force Versus Velocity Measurement

In this research the force measurement is researched in detail; however, the kinematics could also be measured. The advantages/disadvantages of the force vs.

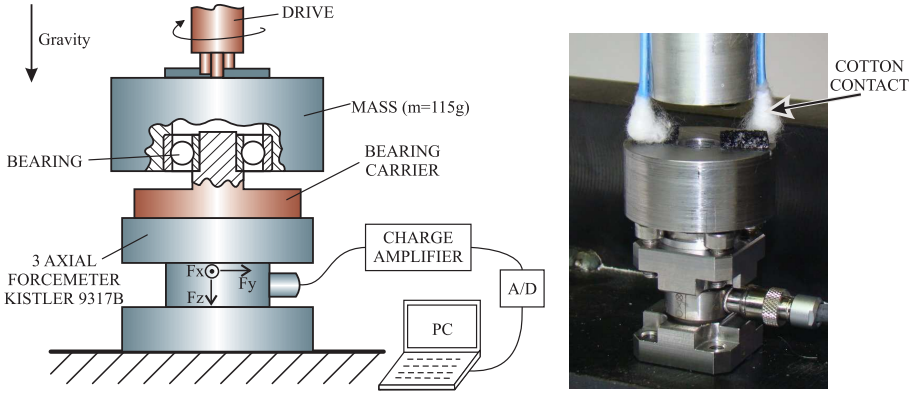

Figure 4: Configuration of the experimental set-up

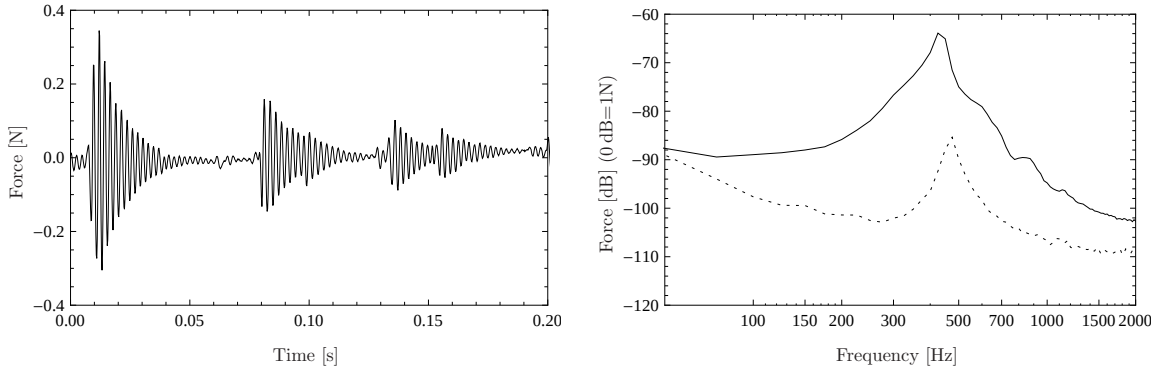

Figure 5: Typical bearing signal: a) raw signal of bearing with axial fault, b) amplitude spectrum: — axial fault, - - - new bearing

the velocity measurement in the case of a fixed attachment to the surroundings are researched in this section, see Figure 6.
Because the natural frequency observed in Figure 5 does not depend on frequency of rotation the drive motor was removed and the hole in the 115g rotating mass was used for the laser beam measurement of the axial velocity of the non-rotating axis, see Figure 6. Radial velocity was measured as shown in Figure 6. The measurement was started after the rotating mass was released from an initial velocity. From Figure 7 it can clearly be seen that the force measurement does measure the natural response at 450Hz while the velocity measurement is much less sensitive (only a small peak in the axial direction can be identified). No higher natural frequencies could be identified in the frequency range up to 10kHz.

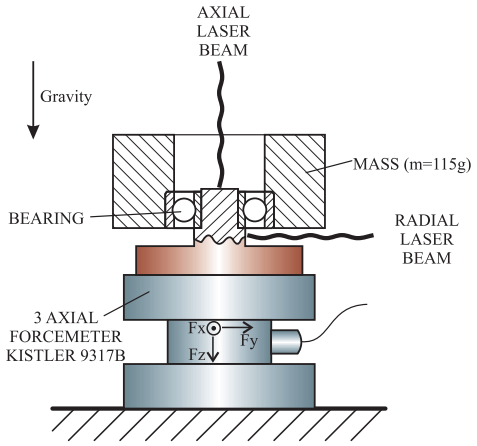

Figure 6: Experimental set-up for force-velocity analysis.

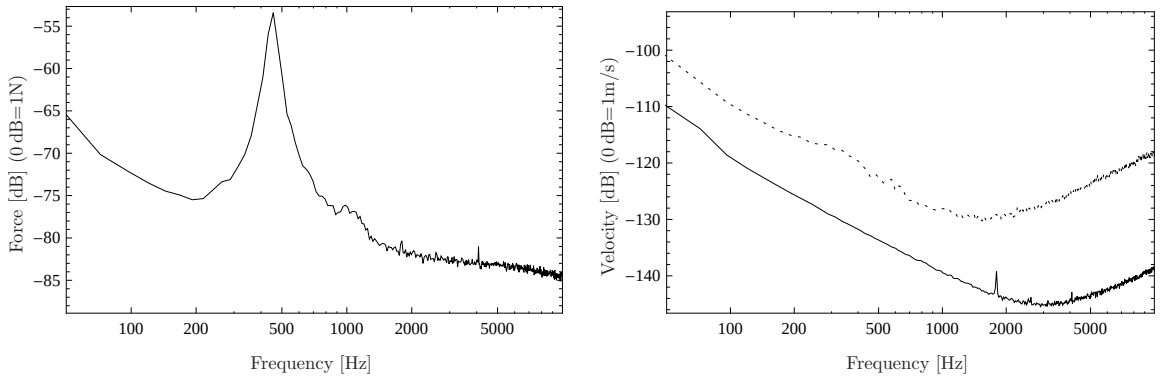

Figure 7: a) amplitude spectrum of force, b) amplitude spectrum of velocity — axial direction, - - - radial direction

3.3 Preparation of the samples

In this research a series of small, radial bearings was investigated, see Table 1. When a bearing leaves the manufacturer's production line it is checked for faults[2] and is fault-free when it arrives at the buyer; however, during installation the bearings can be overloaded or exposed to a harsh environment, which can cause the bearings to become faulty.

The focus of this research was to identify typical installation faults shown in Figure 8. For this investigation some typical mechanical faults were prepared with a tensile-test machine; as shown in Table 2, each mechanical fault was introduced at three levels: low, medium and high. For example, the bearing exposed to a bending moment in the range from 0.8 to 1.0 Nm is (by the manufacturer of the bearings) considered as healthy with a low fault rating. The bearing with a bending moment in the range 1.5 to 2.0 Nm is considered to be at the limit between healthy and faulty (medium fault rating). And the bearing with bending moment in the range > 3 Nm is considered faulty (high fault rating).

The mechanical loads were relatively easy to quantify; however, the samples with the aluminium-dust contamination and the cage deformation were not easy to quantify and were prepared by trial and error.

For each fault rating two different bearing samples were prepared and tested. Because three fault ratings for each fault type were investigated, it follows that, per fault type, 6 samples were prepared. Further, because 5 typical fault types were investigated a total of 30 samples were prepared and tested. Each sample was tested axially prestressed in both directions, consequently the total number of measurements was 60.

Table 1: Bearing geometry, see Figure 1

inner diameter	outer diameter	width	D_b	D_m	θ	N_b
4 mm	12 mm	4 mm	2 mm	7.805 mm	0 deg	7

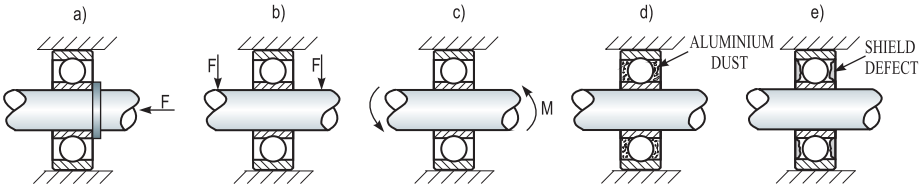

Figure 8: Typical bearing installation faults: a) axial, b) radial, c) bending moment, d) contamination, e) shield defect

[2]By acoustic-noise inspection.

Table 2: Introducing the bearing's mechanical faults, see Figure 8

Fault type	Low	Medium	High
Axial load	650-700 N	1000-1200 N	>1600 N
Radial load	600-650 N	850-1000 N	>1400 N
Bending moment	0.8-1 Nm	1.5-2.0 Nm	>3 Nm

4 Analysis of the fault rating and fault type

As can be seen from the Figure 5b the difference in amplitude spectrum between the faulty and the healthy bearing is large and for the identification of fault rating simple time domain (e.g. peak-to-peak, rms,..., total energy) or frequency domain (maximum amplitude/energy at selected frequency pass) techniques would be successful enough. However, by using envelope analysis more details on the amplitude and frequency of a particular fault type are possible. Therefore, this research focuses on a two-stage bearing-fault analysis. The first stage identifies the rating of the fault and, if the bearing is faulty, then the second stage identifies the type of the fault.

4.1 Fault-rating analysis

The experimental setup (Figure 4) allows testing at various rotating speeds and pre-stresses and also allows an analysis of the force measurements in all three directions. This research focuses on a rotating frequency of 4 Hz and a pre-stress of 115 gram, and a dynamical force in the axial direction of the bearing. According to the dimensions of the tested bearings and the shaft's rotating speed, the characteristic fault frequencies, as defined in Section 2.1, are given in Table 3.

Table 3: Bearing-fault frequencies

f_o	f_i	f_c	f_{bs}	f_{re}
10.4 Hz	17.6 Hz	1.5 Hz	7.3 Hz	14.6 Hz

As these fault frequencies cannot be seen in the spectrum of a raw signal, the envelope detection method was applied for the bearing-condition detection. As discussed in Sections 2.2 and 2.3, the first step of the investigation is spectral filtering around the resonant frequency. Based on the spectrum of the bearing vibration shown in Figure 5b, the frequency band from 300 to 550 Hz was chosen. The step following the filtering is the envelope detection (Figure 3a) and the calculation of its power spectrum (Figure 3b).
Like with Randall [23], the differences in the power spectrum of the envelope on the dB scale were used for the fault-rating identification. The fault-rating identification procedure is as follows:

- the envelope power spectrum is transformed to the dB scale (Figure 9a)[3]
- the maximum value on the dB scale is found
- the difference between the maximum value and the maximum value of the new/healthy bearing is determined

The results for a new bearing and a bearing with a high axial fault rating are shown in Figure 9b). The fault rating can be clearly identified. In this research a fault rating up to 8 dB is considered very healthy, a fault rating in the range 8-20 dB is considered with warnings, while a fault rating exceeding 20 dB is considered dangerous.

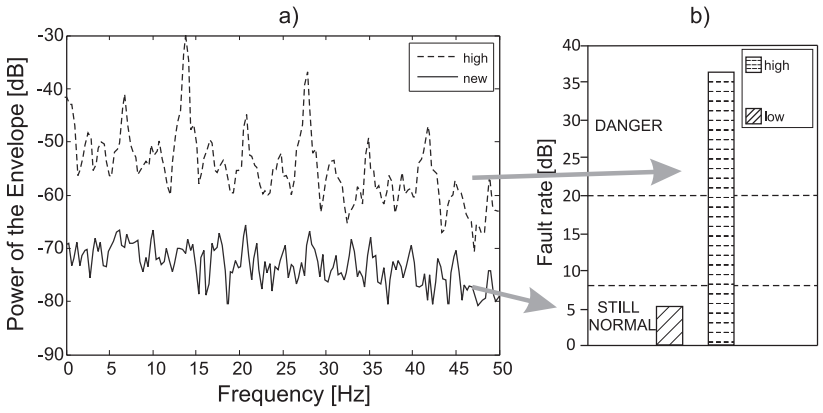

Figure 9: Identification of the fault rating for an axial load: a) dB power spectrum, b) fault rating

By applying the fault-rating procedure to radial, bending moment, contamination and shield faults, Figure 10 is obtained. It is clear that some of the bearings with a low fault rating are identified as dangerous (e.g., radial and contamination). On one hand, this shows that the current (acoustic-noise) method used by the manufacturer of the bearings is maybe not as sensitive to faults as the one proposed here. On the other hand, this shows that the preparation needs to be very careful and is sometimes hard to do (e.g., contamination and cage faults).

4.2 Fault-type analysis

Wang *et al.* [27] first identified the fault type and then the fault rating; in this research it was found to be more reliable to first identify the fault rating and then the fault type. The most reliable fault-type analysis can be made on bearings with a critical fault rating. Figure 11 shows the power spectrum of

[3]In this research 1 N^2 is used for the reference level on the dB scale and the frequency band is selected according to Table 3, where 50 Hz corresponds to approximately $3\times f_i$.

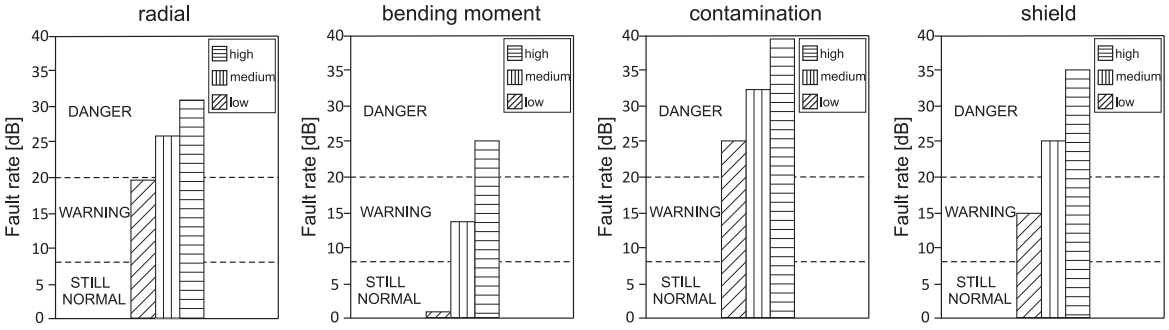

Figure 10: Fault rating for the different typical faults

the envelope for all five investigated fault types with a critical fault rating; the dashed lines define the characteristic bearing-fault frequencies (see Table 3).
A detailed analysis of different bearings showed that the axial bearing fault can be identified at the rolling element frequency f_{re}. The ball-bearing frequency can also be identified in the bending moment and contamination bearing faults; however, additionally, the bending moment and contamination have increased amplitudes at the frequency of the inner raceway f_i, and the contamination fault differs from the bending moment in an increased broadband response. The radial fault was found to have increased amplitudes at the inner f_i and outer f_o frequencies and also at the ball spin frequency f_{bs}. The shield fault was found to be represented by the frequency of the outer raceway f_o.
Table 4 gives details of the correlation of the bearing fault and the characteristic bearing frequencies.

Table 4: Bearing fault frequencies

Fault type	f_o	f_i	f_c	f_{bs}	f_{re}
axial					√
radial	√	√		√	
bending moment		√			√
contamination		√			√
shield	√				

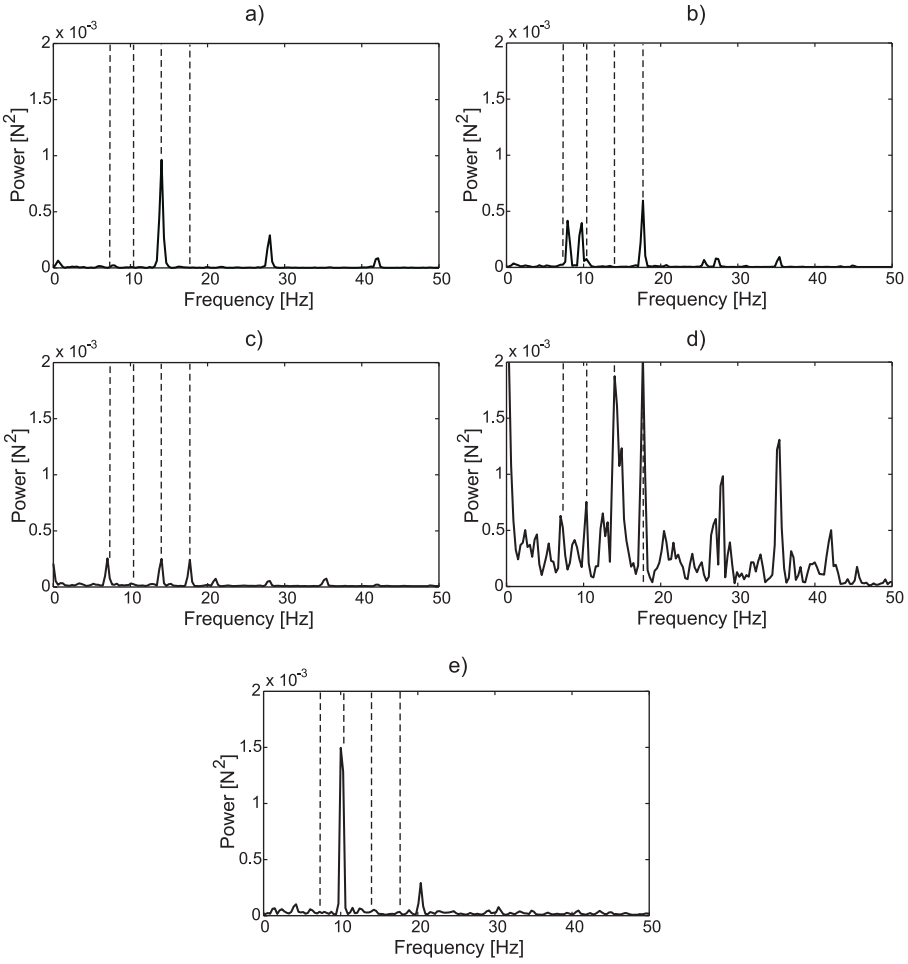

Figure 11: Envelope power spectrum for: a) axial load, b) radial load, c) bending moment load, d) contamination and e) shield defect

5 Conclusion

In this paper, a bearing-fault detection method based on a force measurement and the envelope-detection method is presented. This research started because in real-life applications acceleration/velocity-based techniques have several drawbacks: the acceleration/velocity sensor measures the surface vibration at a given location of the sample; the amplitude and the frequency depend on the sensor location as well as on the boundary condition. The problem, therefore, is twofold: the sensor measures the local structural vibrations and the measured amplitudes in the frequency domain can differ a great deal, even for

the same sample. To avoid the interaction with the surroundings ideally a free-free fixation is needed; because the sample (e.g., an electric-motor) needs to be tested under operating conditions the free-free fixation is hard to achieve in real-life applications. As the boundary conditions alter the vibration response, this influences the vibration response and therefore the fault identification.
On the other hand, a force-based measurement requires fixation to a rigid surrounding, with the force sensor positioned at the intersection. In this way the boundary conditions are easier to control and the structurally borne vibrations due to the bearing faults are easily measured. This research shows that a frequency-domain analysis can successfully be applied to identify the amplitude as well as the frequency of the force signals.
Five typical bearing faults that are possible during the assembly process were systematically researched and the relatively simple envelope-based signal processing was successful in identifying the fault rating as well as the fault type.
The presented procedures were also successfully applied to a high-series production line.

Acknowledgements

We would like give special thanks to Robert Randall, Professor at School of Mechanical & Manufacturing Engineering, UNSW Sydney, Australia, for his valuable suggestions on this research.

The support provided to the second author by the EU Marie Curie Actions in the form of programme Advanced and New SImulation Methods in Vehicle VIbro-Acoustics (SIMVIA2) is deeply appreciated.

References

[1] P.J. Kim and I.R.G. Love. A review of rolling element bearing health monitoring. pages 145–154, Houston, TX, 19-21 April 1983. Vibration Institute, In Proceedings of Machinery Vibration Monitoring and Analysis Meeting.

[2] N. Tandon and A. Choudhury. A review of vibration and acoustic measurement methods for the detection of defects in rolling element bearings. *Tribology International*, 32(8):469–480, 1999.

[3] D. Ho and R. B. Randall. Optimisation of bearing diagnostic techniques using simulated and actual bearing fault signals. *Mechanical Systems and Signal Processing*, 14(5):763–788, 2000.

[4] P.D. McFadden and J.D. Smith. Vibration monitoring of rolling element bearings by the high-frequency resonance technique – a review. *Tribology International*, 17(1):3–10, 1984.

[5] P. D. McFadden and J. D. Smith. Model for the vibration produced by a single point defect in a rolling element bearing. *Journal of Sound and Vibration*, 96(1):69–82, 1984.

[6] P.D. McFadden and J.D. Smith. The vibration produced by multiple point defects in a rolling element bearing. *Journal of Sound and Vibration*, 98(2):263–273, 1985.

[7] Y.-T. Su and S.-J. Lin. On initial fault detection of a tapered roller bearing: Frequency domain analysis. *Journal of Sound and Vibration*, 155(1):75–84, 1992.

[8] Y. Yang, D. Yu, and J. Cheng. A fault diagnosis approach for roller bearing based on IMF envelope spectrum and SVM. *Measurement*, 40(9-10):943–950, 2007.

[9] L. Guo, J. Chen, and X. Li. Rolling Bearing Fault Classification Based on Envelope Spectrum and Support Vector Machine. *Journal of Vibration and Control*, 15(9):1349–1363, Sep. 2009.

[10] Y.-T. Sheen. An analysis method for the vibration signal with amplitude modulation in a bearing system. *Journal of Sound and Vibration*, Volume 303(Issue 3-5):Pages 538–552, 20 June 2007.

[11] R. B. Randall. Detection and diagnosis of incipient bearing failure in helicopter gearboxes. *Engineering Failure Analysis*, 11(2):177–190, 2004.

[12] E. Mendel, T.W. Rauber, F.M. Varejao, and R.J. Batista. Rolling element bearing fault diagnosis in rotating machines of oil extraction rigs. Glasgow, Scotland, August 2009. 17th European Signal Processing Conference, EURASIP, 2009.

[13] D.M. Yang, A.F. Stronach, and P. MacConnell. The application of advanced signal processing techniques to induction motor bearing condition diagnosis. *Meccanica*, 38(2):297–308, 2003.

[14] W.J. Wang, Z.T. Wu, and J. Chen. Fault identification in rotating machinery using the correlation dimension and bispectra. *Nonlinear dynamics*, 25(4):383–393, August 2001.

[15] M Boltežar and J Slavič. Fault detection of dc electric motors using the bispectral analysis. *Meccanica*, 41(3):283–297, June 2006.

[16] M. Boltežar, I. Simonovski, and M. Furlan. Fault detection in dc electro motors using the continuous wavelet transform. *Meccanica*, 38(2):251–264, 2003.

[17] W. Bao, R. Zhou, J. Yang, D. Yu, and N. Li. Anti-aliasing lifting scheme for mechanical vibration fault feature extraction. *Mechanical Systems and Signal Processing*, 23(5):1458–1473, 2009.

[18] W. Su, F. Wang, H. Zhu, Z. Zhang, and Z. Guo. Rolling element bearing faults diagnosis based on optimal morlet wavelet filter and autocorrelation enhancement. *Mechanical Systems and Signal Processing*, 2009.

[19] X. Wang, Y. Zi, and Z. He. Multiwavelet denoising with improved neighboring coefficients for application on rolling bearing fault diagnosis. *Mechanical Systems and Signal Processing*, 2010.

[20] S. Abbasion, A. Rafsanjani, A. Farshidianfar, and N. Irani. Rolling element bearings multi-fault classification based on the wavelet denoising and support vector machine. *Mechanical Systems and Signal Processing*, 21(7):2933–2945, 2007.

[21] C. Castejon, O. Lara, and J.C. Garcia-Prada. Automated diagnosis of rolling bearings using mra and neural networks. *Mechanical Systems and Signal Processing*, 24(1):289–299, 2010.

[22] M Artes G N Marichal and J C Garcia-Prada. An intelligent system for faulty bearing detection based on vibration spectra. *Journal of Vibration and Control*, 2010.

[23] R. B. Randall. State of the art in monitoring rotating machinery - part 1. *Sound and Vibration*, 38(3):14–21, 2004.

[24] Braun S. *Discover signal processing: An interactive guide for engineers.* John Wiley & Sons, Ltd, 2008.

[25] R. Yan and R.X. Gao. Multi-scale enveloping spectrogram for vibration analysis in bearing defect diagnosis. *Tribology International*, 42(2):293–302, 2009.

[26] S.L. Hahn. *Hilbert transforms in signal processing.* Artech House, 1996.

[27] G.F. Wang, Y.B. Li, and Z.G. Luo. Fault classification of rolling bearing based on reconstructed phase space and gaussian mixture model. *Journal of Sound and Vibration*, 323(3-5):1077–1089, 2009.